communications medicine

A Nature Portfolio journal

Article

https://doi.org/10.1038/s43856-025-00834-6

Locating eloquent sites identified during brain tumor intraoperative mapping on reference MRI atlas

Angela Elia[1,2], Alexandre Roux[1,2], Clément Debacker[2], Sylvain Charron[2], Giorgia Simboli[1,2,3], Alessandro Moiraghi[1,2], Bénédicte Trancart[1], Edouard Dezamis[1], Jun Muto[4], Fabrice Chretien[3], Marc Zanello[1,2], Catherine Oppenheim[2,5] & Johan Pallud[1,2]

Abstract

Background Correlating the human connectome with clinical responses elicited during intraoperative brain mapping helps understanding of the intrinsic organization of the human brain. Methods for locating eloquent sites on neuroimaging are not standardized. In the present study, we standardized a methodology for locating subcortical eloquent sites identified during intraoperative mapping for awake brain tumor resection on a reference brain template.

Methods Subcortical eloquent sites were tagged by co-registration of intraoperative photographs with early postoperative MRI (< 48 h). Neuroimaging data were normalized into MNI152 space. To assess whether the location of subcortical eloquent sites on the MNI template was concordant with the expected brain connectivity, we compared each subcortical eloquent site with the Human Connectome Project 1065 probabilistic tractography atlas.

Results We analyze 290 subcortical eloquent sites identified during 69/90 awake surgeries. 2/290 (0.7%) subcortical eloquent sites identified intraoperatively do not intersect with a fiber tract according to the reference atlas. Among the other 288 that successfully intersect with, at least, one white matter tract, 255/288 (88.5%) have a clinical response elicited intraoperatively that is congruent with the intersected white matter tract. In the remaining 33/288 (11.5%) functional incongruent and the 2/290 (0.7%) anatomical incongruent subcortical sites, the minimal mean distance between the eloquent site and a congruent with matter tract is 3.6 ± 4.4 mm (range 1.0–23.9, median 3.6, interquartile range 2.5–5.4).

Conclusions We propose a standardized methodology to locate with accuracy on a reference brain template subcortical eloquent sites identified intraoperatively during functional brain mapping using direct electrical stimulations under awake condition.

Plain language summary

Specific areas of the brain are known to enable particular functions, resulting in people being at risk of disability if these areas are injured. We aimed to establish a reliable method to accurately locate these sites during surgery in people with brain tumors while they are awake. We used photographs taken during the surgery and brain scans taken soon after surgery to match the sites with a template of the brain. We found that nearly all the areas we identified sites matched parts of the brain known to enable particular functions, suggesting our method is accurate. This standardized approach could improve our understanding of the human brain and enable better treatment of people with brain cancer that enables them to avoid disabilities developing.

The use of direct electrical stimulations under awake conditions is an accurate intraoperative tool for the causal mapping of brain functions during brain tumor surgery[1–10]. It is currently considered the gold standard brain mapping technique to achieve maximal safe resection by minimizing brain damages for neurosurgical purpose[1,2,4,11–19].

In addition, for research use, and with the full knowledge of the theoretical limitations[20,21], direct electrical stimulations under awake conditions help understanding brain function[20,22–27]. These methods offer insights regarding individual brain connections and identify critical eloquent structures, i.e. generating permanent deficits if damaged[20,28]. Therefore, correlating eloquent structures identified intraoperatively using direct electrical stimulations to human connectome MRI reference atlas, offers a unique insight into the organization of the human brain. Several groups studied brain functioning by correlating direct electrical stimulations with

[1]Service de Neurochirurgie, GHU Paris Psychiatrie et Neurosciences, Site Sainte Anne, F-75014 Paris, France. [2]Université Paris Cité, Institute of Psychiatry and Neuroscience of Paris, INSERM U1266, F-75014 Paris, France. [3]Service de Neuropathologie, GHU Paris Psychiatrie et Neurosciences, Site Sainte Anne, F-75014 Paris, France. [4]Department of Neurosurgery, Fujita Health University, Aichi, Japan. [5]Service de Neuroradiologie, GHU Paris Psychiatrie et Neurosciences, Site Sainte Anne, F-75014 Paris, France. e-mail: johanpallud@hotmail.com; j.pallud@ghu-paris.fr

neuroimaging[27,29,30]. However, studies assessing the integration of deep subcortical eloquent sites identified intraoperatively on reference MRI templates remain scarce and the methodologies were not detailed, homogenized, or standardized among groups. Particularly, the use of intraoperative neuronavigation systems based on pre-operative MRI to locate subcortical eloquent sites is impaired by inherent biases induced by intraoperative brain shift[31].

Here, we hypothesized that co-registering subcortical eloquent sites located in the depth of the surgical cavity and captured on intraoperative photographs with early postoperative MRI will help control the brain shift induced by surgical resection.

The aims of the present study were to develop a standardized methodology for locating subcortical eloquent sites identified intraoperatively using direct electrical stimulations during awake brain mapping on a reference MRI brain atlas and to evaluate its accuracy by comparing the congruence of subcortical eloquent sites with the Human Connectome Project (HCP) 1065 probabilistic tractography atlas. To improve validity and reproducibility, we selected a homogeneous group of adult patients harboring the same supratentorial *isocitrate dehydrogenase (IDH)*-mutant glioma.

This study analyzed 90 patients with *IDH*-mutant diffuse glioma who underwent awake surgery with functional brain mapping. The mapping identified 290 eloquent sites in 69 patients (76.6%). Of the 290 subcortical sites, 99.3% intersected with at least one white matter fiber tract, with 88.5% showing functional congruence. Results supports that this standardized approach has high accuracy in identifying functionally relevant brain regions.

Materials and methods

Dataset

We performed an observational, retrospective, and consecutive cohort study at a single tertiary referral neurosurgical center, between September 2021 and March 2023. The screening criteria were: 1) adult patients; 2) supratentorial *IDH*-mutant glioma according to the 2021 World Health Organization classification of tumors of the Central Nervous System[32]; and 3) function-based resection with intraoperative functional brain mapping using direct electrical stimulations under awake condition.

The study protocol was approved by the local institutional review board (Collège de Neurochirurgie IRB00011687, IRB#1:2023/02). An informed written consent was obtained from all patients prior to enrollment.

Intraoperative data acquisition

A reproducible "asleep-awake-asleep" surgical protocol was used by the same senior neurosurgeon, as previously detailed[2,4,5,33,34]. The intraoperative functional brain mapping was performed by cortical and subcortical direct electrical stimulations during the awake phase of surgery. A bipolar electrode (5 mm interspace between tips) was used and a biphasic current (pulse frequency 60 Hz; phase duration 1 ms; Osiris NeuroStimulator, Inomed, Emmendingen, Germany) was applied. The current intensity was determined by stimulating the sensory/motor area with a progressive amplitude increase (baseline 1 mA, 0.5 mA increments) until reproducible positive responses were elicited. The same current intensity served for both cortical and subcortical functional mappings. All events were recorded on a clinical basis by a senior speech therapist who directly checked neurological and cognitive functions through defined and reproducible intraoperative tasks previously reported[4,35](Supplementary Table 1). The whole exposed brain was tested. Each site eliciting a similar clinical response three times following nonconsecutive stimulations was considered eloquent, reported on intraoperative records, and marked with a sterile numbered 5-mm squared tag. The resection was performed together with direct electrical stimulations for subcortical functional mapping while the awake patient was performing the required tasks. Resection was stopped when subcortical eloquent structures were identified within the surgical cavity (no security margin between resection limits and identified eloquent structures[36]) or until the patient felt too tired to work efficiently[2]. Intraoperative 2D photographs of the surgical field were taken after initial cortical mapping and at the end of the resection to capture all tagged eloquent cortical and subcortical sites in one or two photographs treated as two independent images.

Magnetic Resonance Imaging acquisition

Early postoperative MR images were obtained within the first postoperative 48 h and using 1.5-Tesla (Signa EchoSpeed, General Electric Healthcare, Milwaukee, Wisconsin, USA). 3D T1-weighted sequences with and without gadolinium injection (slice thickness 1.2 mm, repetition time ranging 10.216–11.192 ms, echo time ranging 3.356–4.200 ms) were selected from the Picture Archiving and Communication Clinical System. Images were pseudonymized based on an alphanumeric-coded patient-identification system and converted into Neuroimaging Informatics Technology Initiative (NIfTI) using the Statistical Parametric Mapping 12 toolbox (SPM12 - Functional Imaging Laboratory, The Wellcome Trust Center for Neuroimaging – Institute of Neurology, University College London, UK) on the MATrix LABoratory (R2018a; MathWorks, Natick, Massachusetts, USA) programming and scientific computing language.

Preprocessing neuroimaging data

Neuroimaging data from early postoperative MR images were preprocessed using open-source Multi-Image Analysis GUI software (2019, MANGO software, version 4.1; Research Imaging Institute, University of Texas Health Science Center, San Antonio, USA, http://ric.uthscsa.edu/mango/) by the reference investigator along three consecutive steps (Fig. 1): 1) removing the non-brain tissues (skull, scalp, and other extraneous structures) using the "Brain Extract Tool" plugin (0.5 intensity threshold and a 0.0 threshold gradient); 2) visual adjustment of the pixel intensity values to optimize the greyscale resolution contrast between cortical and subcortical structures (i.e. clear contrast between cortex in grey and subcortical structure in white as illustrated in Fig. 1 and detailed in Supplementary table 2); 3) volume rendering of the brain surface using the "Build Surface" option retaining the default parameters in most of cases on the whole brain without excluding the surgical cavity. In cases of artefacts, parameters have been modified by trial and error to obtain the proper combination and a satisfactory 3D brain reconstruction. In details, "Surface threshold" to control the image intensity, "Shrink-wrapping option" to reduce internal surface data, "Image smoothing" to adjust the surface noise, "Resolution" to control the surface resolution, "Surface smoothing" to remove redundant or not-contributing surface points, were adjusted as required.

Co-registration of intraoperative photographs with neuroimaging data

The co-registrations of intraoperative 2D photographs with the 3D brain reconstruction were manually performed by the reference investigator along four consecutive steps (Fig. 1): 1) the 3D brain reconstruction was set on the same scale, position, and orientation to those of the photographs; 2) free Vitrite software (version 1.1 for Windows by Ryan VanMiddlesworth) was then used to set transparency of the photographs and the 3D brain reconstruction to allow proper overlay; 3) the 3D model was then aligned with the photographs using all visible and recognizable anatomical landmarks (vessels, sulci, falx, tentorium, ventricles, basal ganglia, borders of the resection cavity) and applying different blending levels to control how the photograph and the 3D model overlayed; 4) a specific Region Of Interest (ROI) of 1 mm in diameter was placed and tagged at the center of the numbered 5-mm squared tag positioned at all subcortical eloquent sites that were identified on intraoperative photographs within the white matter. In cases of two intraoperative photographs taken in the same patient to capture all subcortical eloquent sites, the procedure was repeated on each photograph. Each ROI was saved as a NIfTI file.

Normalization of subcortical eloquent sites

To locate a subcortical eloquent site on each patient's MRI scan within a reference MRI brain atlas, we first normalized the individual postoperative MRI to the template space, obtaining a corresponding deformation field.

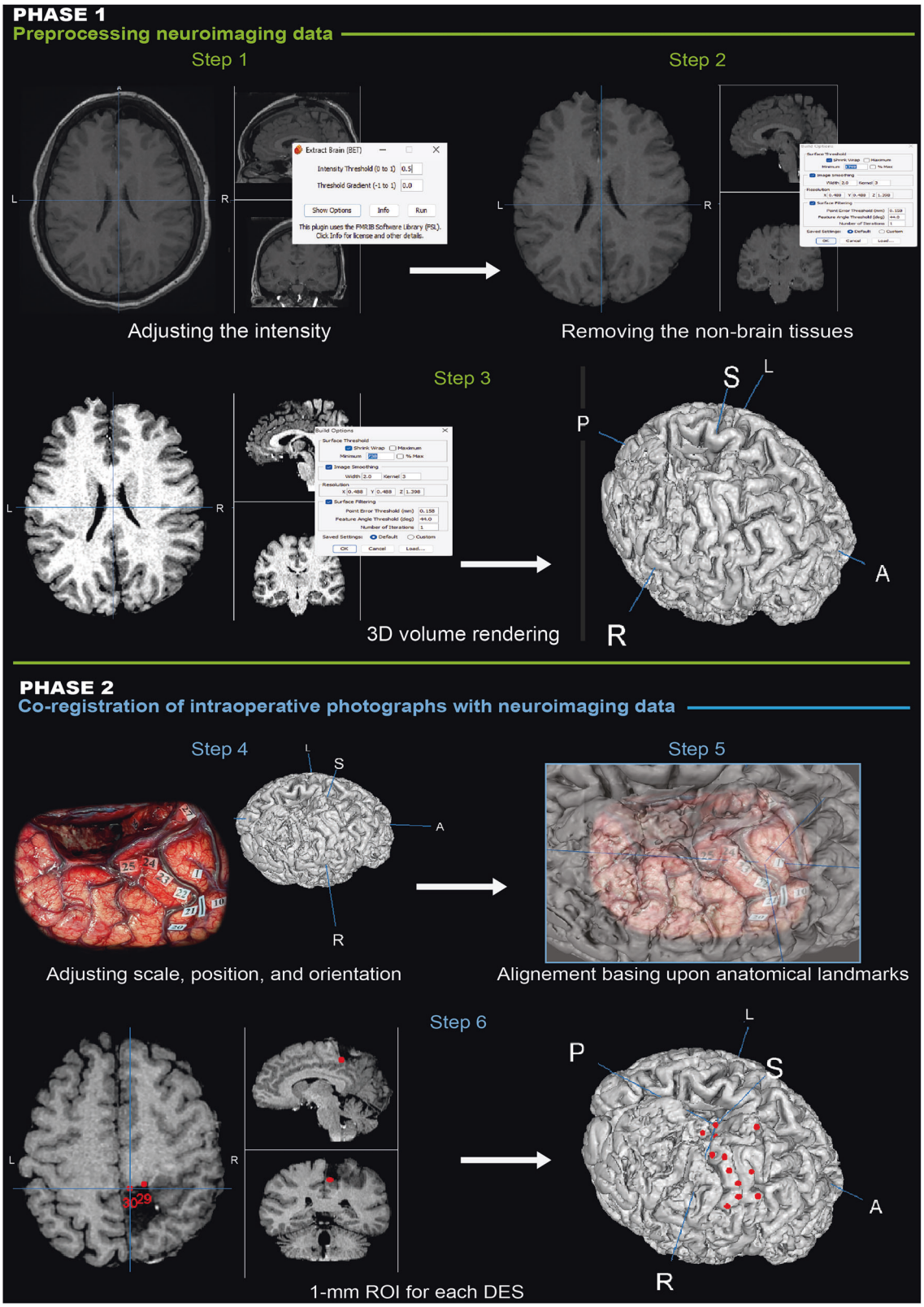

This deformation field encapsulated the spatial transformation required to map individual anatomical features onto the template. Once normalization was complete, the deformation field was applied to the coordinates of the subcortical eloquent site of interest, transforming its location from the native space to the standardized template space. The normalizations of neuroimaging data were performed by the reference investigator using SPM12 - Clinical Toolbox and specifically the "Segment" and "Normalise: Write - Dependency" functions[37]. The segmentation algorithm, based on Tissue Probability Maps, generated a probabilistic map through the segmentation of different brain tissues (including gray matter, white matter, cerebrospinal fluid) comparing the intensity and spatial characteristics of each voxel. Tissue Probability Maps based on the Montreal Neurological Institute

Fig. 1 | Step-by-step process to locate brain subcortical eloquent sites on postoperative MRI. The process to locate subcortical eloquent sites identified intraoperatively during awake brain mapping on postoperative MRI consists of two phases: PHASE 1. Preprocessing neuroimaging data. Step 1: Neuroimaging Informatics Technology Initiative (NIfTI) files were uploaded on the Multi-Image Analysis GUI (MANGO) software and the Brain Extract Tool plugins was used to remove non-brain tissues (skull, scalp, and other extraneous structures) using an intensity threshold of 0.5 and a gradient threshold of 0.0; Step 2: the intensity of the pixel values was adjusted to optimize the contrast between cortical and subcortical structures; Step 3: the "Build Surface" of the MANGO software was then used to create the surface rendering with the default parameters; in cases of poor-quality volume rendering, the parameters were adjusted according to the neuroimaging characteristics until a good quality 3D brain model is obtained. PHASE 2. Co-registration of intraoperative photographs with neuroimaging data. Step 4: the 3D brain model was set on the same scale, position, and orientation than those of the 2D photographs; Step 5: the 3D model was aligned with the photographs using all visible and recognizable anatomical landmarks (vessels, sulci, falx, tentorium, ventricles, basal ganglia, borders of the resection cavity) and applying different blending levels to visually control how the 2D photograph and the 3D model overlayed using the Vitrite software; Step 6: a specific Region Of Interest (ROI) of 1 mm in diameter was placed and tagged at the center of the numbered 5-mm squared tag positioned at each subcortical eloquent site identified intraoperatively in the white matter. *A: anterior; L: left; R: right; ROI: region-of-interest; S: superior*.

(MNI) 152 template provided by the SPM12 Clinical toolbox were used as reference maps to guide the alignment of individual brain images (Supplementary fig. 1). To unify the normalization process and to ensure that the forward warp was used to transform neuroimaging data from native space into the standard MNI space, the two functions, "Segment" and "Normalise: Write", were combined in the same batch editor (Supplementary Fig. 2). In the "Segment" function, we changed the parameter of bias control into "Save Bias corrected" and we set the "Deformation field" parameter into "Forward". Then, in the "Normalise: write" function we set the "Deformation field" as dependent on the "forward Deformation" and the Image to write as dependent on the "Segment: Bias corrected". The Clinical Toolbox "Segment Function" allowed lesion masks to exclude regions of interest (the tumor area for instance) from affecting the estimation of tissue probabilities or improving segmentation accuracy by focusing on non-lesioned tissues. In addition, the "Normalise: Write – Dependency" function normalized the segmented tissues to a standard template space (e.g., MNI space) while maintaining alignment with the pathological anatomy. So it uses the deformation fields generated during segmentation to write the normalized images and to ensure consistency between the native image space and the normalized template space.

Finally, we adjusted the parameters of the Bounding Box that define the analysis area borders from the anterior commissure. We used the setting (−90 −126 −72; 90 90 108) as previously reported[38]. To ensure a sufficient resolution, a 1 mm voxel size was applied for all normalized MRI. We then obtained a deformation field image that stored the transformation parameters and mapped the individual subject's brain image to the template space. The inverse deformation field was calculated through a specific script (Supplementary Fig. 3). This allowed applying the same transformation to the ROI and obtaining their template-space coordinates for each subcortical eloquent site.

Validation of the location of subcortical eloquent sites identified intraoperatively

Following 3D brain reconstruction and alignment, all cases were qualified by the reference investigator as (Supplementary fig. 4): "Good": accurate 3D brain and resection cavity reconstruction without artefacts and with a perfect alignment of all available anatomical landmarks; "Medium": sufficient 3D brain reconstruction with few artefacts and a sufficient alignment based on all but one or two available anatomical landmarks; "Poor": insufficient 3D brain reconstruction with many artefacts and an alignment based on a maximum of two available anatomical landmarks. All cases were then reviewed with a second investigator to validate the identification of anatomical landmarks, the overlaying results, and the location of each subcortical eloquent site identified intraoperatively.

Hybrid quality assessment

To assess the accuracy of the normalization process, the reference investigator performed a qualitative visual inspection of the proper co-registration between the normalized MRI and the MNI template. The template was overlapped to the normalized image using MANGO software and the matching of different anatomical structures was visually checked. We then performed a quantitative analysis by evaluating the agreement between the blinded evaluators' identification of the same points on normalized brains. Two different experimented evaluators identified nine predefined reference points on a random sampling of 18 normalized patient brains (Supplementary data 1). We then calculate the mean distance between the MNI template and normalized patient brains, as previously reported[11,38]. We adapted a Python script, previously reported[11,38], to the dataset allowing the automated comparisons among the MNI reference coordinates and the normalized ones (Supplementary Fig. 5). This distance evaluated the gap deformation of the residual cerebral parenchyma after the normalization procedure: the lower the mean distance, the better the co-registration between the normalized images and the reference space in the MNI template.

Comparison between subcortical eloquent sites identified intraoperatively and brain tractography atlas

To assess whether the location of subcortical eloquent sites identified intraoperatively on the normalized MNI template were congruent with the expected brain connectivity, we compared each eloquent site to the homolateral probabilistic tractography. The clinical response elicited intraoperatively at each subcortical eloquent site was correlated to the specific white matter fiber tracts sustaining the brain function to check for functional correspondence. If the clinical response elicited intraoperatively was consistent with the identified white matter fiber tract, the correlation was considered valid and the ROI corresponding to the subcortical eloquent site was considered properly located on normalized MNI template. We used the Human Connectome Project (HCP) 1065 probabilistic tractography atlas, which resulted from 1065 subject's tractography normalized in the International Consortium for Brain Mapping (ICBM) 2009a Nonlinear Asymmetric space[39]. The ICBM2009a template and all white matter fiber tracts have been aligned to the MNI152 template provided by the SPM12 toolbox using the procedure used for neuroimaging data processing described above.

To facilitate the analysis, the different distinct subdivisions of the cingulum, the corticopontine tract, the corticostriatal tract, the superior longitudinal tract, and thalamic radiation given in HCP probabilistic tract atlas, were considered all in one for each tract. The overall fiber tract was obtained through the addition of all the distinct subdivisions performed through SPM12. Additionally, due to the probabilistic nature of the fiber tract atlas and several factors affecting the accurate localization of each subcortical eloquent site during the functional mapping (i.e type of probe, pulse frequency, amplitude and polarity, phase, orientation of stimulation, probe geometry and tissue conductivity, brain parenchyma deformation, and the interaction between the glioma and fiber tracts), we set a low cutoff at 0.01 to include a maximum of voxels in each tract to improve the sensitivity of the intersection analysis. This allowed reducing the risk of false negative inherent to the wide variability of the stimulation parameters of each subcortical eloquent site identified intraoperatively. To verify that this cutoff does not significantly affect the specificity of the methodology and so the number of false positive we performed a complimentary analysis applying both a cutoff at 0.05 on a randomized sample.

The correlation between the ROIs of each subcortical eloquent site identified intraoperatively, and the probabilistic tractography atlas, was

Table 1 | Clinical and imaging characteristics of included patients harboring a supratentorial diffuse *IDH*-mutant glioma (*n* = 90)

Parameters	*n*	%
Sex		
Male	53	58.89
Female	37	41.11
Age, years (median, mean ± SD, range)	41.5, 42.35 ± 13.30 (21–74)	
Handedness		
Right	82	91.11
Left	7	7.78
Ambidexter	1	1.11
Preoperative KPS score (median, mean ± SD, range)	100, 96.22 ± 8.29 (60–100)	
Preoperative KPS score		
≤70	4	4.44
>70	86	95.56
Epileptic seizure at surgery		
Yes	74	82.22
No	16	17.78
Neurological focal deficit at surgery		
No	73	81.11
Yes	17	18.89
Neurocognitive deficit at surgery		
No	19	21.11
Yes	71	78.89
Tumor side		
Right	36	40.00
Left	53	58.89
Bilateral	1	1.11
Main tumor location		
Frontal	47	52.22
Temporal	14	15.55
Parietal	14	15.55
Insular	15	16.68
Contrast enhancement		
Yes	36	40.00
No	54	60.00
Type of contrast enhancement		
Faint and patchy	19	21.11
Nodular-like	16	17.78
Ring-like	1	1.11
Tumor volume at surgery, cm^3 (median, mean ± SD, range)	61.78, 44.99 ± 45.56 (6.34–191.34)	

automatized using a composed multi-step MATLAB script (Supplementary Fig. 3). For each ROI, the coordinates in the anatomical space were translated into the MNI 152 space using the inverse deformation field. For each normalized ROI, a spheric mask of 2.5 mm in radius was created and the corresponding voxels were intersected with the voxels of all fiber tracts homolateral to the tumor side using an automatized loop process script, screening all white matter fiber tracts and all identified subcortical eloquent sites in all patients. In case of an intersection (defined as ≥1 overlapped voxels), the script returned a results file reporting the number of voxels intersecting both the white matter tract and the ROI, the intersected tracts, and the corresponding subcortical eloquent site identified intraoperatively. In the absence of intersection, the script returned a results file reporting the minimal distances between the ROI and white matter fiber tracts. In addition, to allow the visual control of the procedure, the corresponding image of the spheric mask and of the intersected white matter fiber tracts, were co-registered and overlapped onto the MNI template.

Statistics and reproducibility

Statistical analyses were conducted using JMP 16 software (SAS Institute Inc., Cary, NC, USA). Data was analyzed using appropriate statistical tests based on the nature of the studied variables: continuous variables were described as mean ± standard deviation (SD); group comparisons were performed using t-tests for normally distributed data or Mann-Whitney U tests for non-parametric distributions; categorical data were summarized as frequencies and percentages while the comparisons were made using the Chi-square test or Fisher's exact test as appropriate. A *p*-value of less than 0.05 was considered statistically significant.

To ensure the reproducibility of our experiments, the sample size calculations were performed a priori based on anticipated effect sizes and variability, aiming for statistical power of at least 80%. Replicates were defined based on the experimental setup, with multiple measurements taken from different patients for each condition (e.g., multiple regions of interest in the brain were analyzed per patient). For neuroimaging data, the normalization process was carefully controlled and validated by different investigators to confirm the reliability of the results. Error bars in the figures represent standard errors of the mean for continuous variables or 95% confidence intervals (CI) where applicable.

Reporting summary

Further information on research design is available in the Nature Portfolio Reporting Summary linked to this article.

Results

Study population

Patient characteristics are detailed in Table 1. During the study period, 90 adult patients harboring an *IDH*-mutant diffuse glioma who underwent a function-based resection with intraoperative functional brain mapping using direct electrical stimulations under awake conditions were included (58.9% men; mean age of 42 ± 13 years, range 21–74).

Intraoperative functional data during awake surgery

All 90 patients were cooperative and a function-based resection based on eloquent sites identified intraoperatively together with the identification of vascular and anatomical boundaries was completed in all cases[11]. The subcortical functional brain mapping (mean current intensity, 3.4 ± 1.0 mA) identified 290 reproducible subcortical eloquent sites (182 and 102 in the left and right hemispheres, respectively; mean 5 ± 3 subcortical eloquent sites per patient, range 1–14) in 69/90 patients (76.6%) (Fig. 2). In the remaining 21 patients, resection was stopped before the identification of subcortical eloquent sites in the depth of the surgical cavity (identification of anatomical and vascular boundaries in 19 cases and increasing spontaneous rate of errors during intraoperative tasks precluding the identification of functional deep limits of resection in two cases).

Quality assessment of the normalization procedure

Early postoperative MRI were performed at a mean 1.3 ± 1.4 postoperative days (range 0-2, median 1, interquartile range 1-1; day-0, *n* = 2, 2.2%; day-1, *n* = 69, 76.7%; day-2, *n* = 19, 21.1%). No manual corrections had to be made in the spatial normalization procedures. The mean distance between normalized images and reference MNI template was 2.8 ± 5.8 mm (range 0–60, median 2, interquartile range 1–2.82).

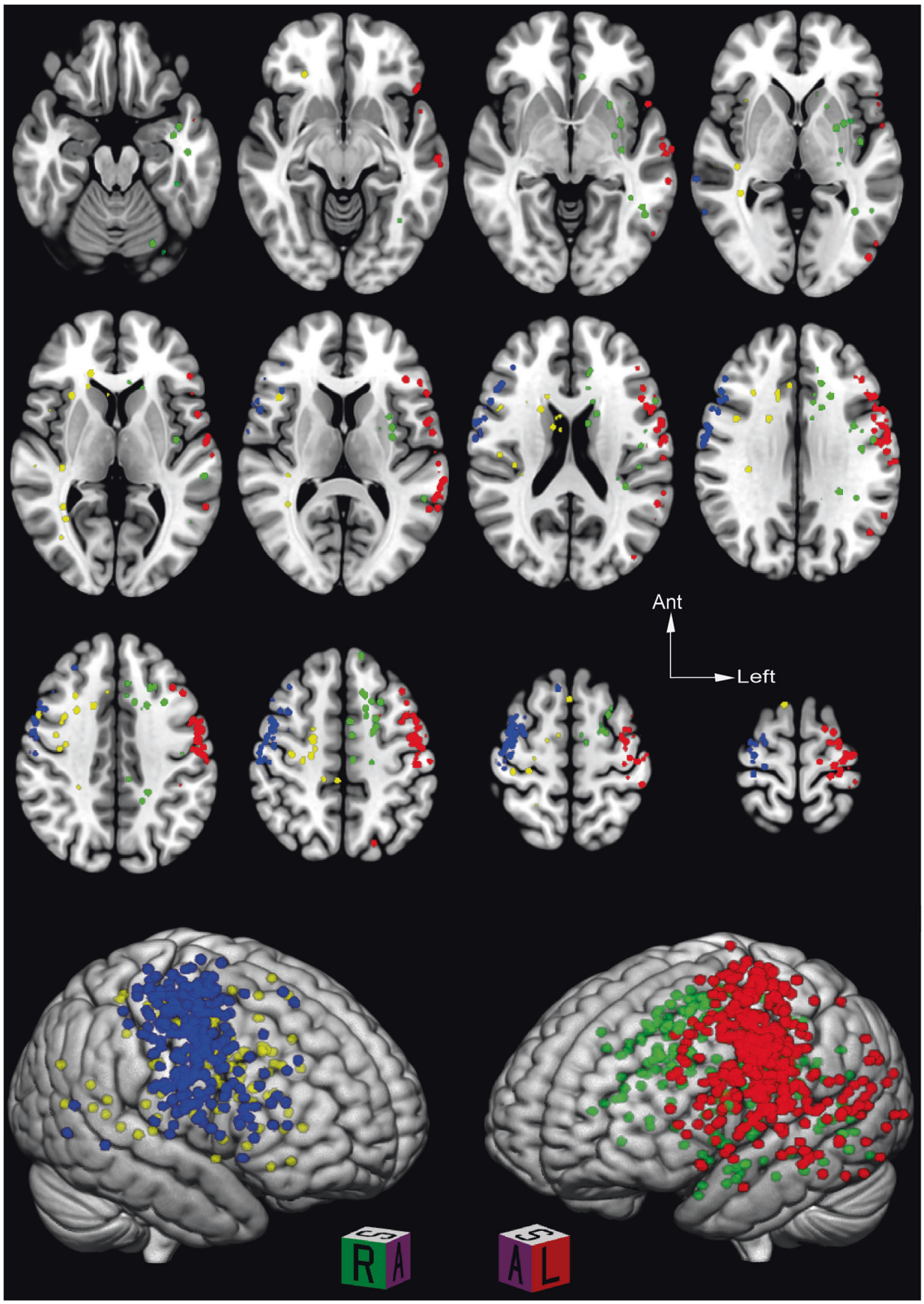

Fig. 2 | Overview of all subcortical eloquent sites identified intraoperatively during awake brain mapping ($n = 290$). During intraoperative functional mapping with direct electrical stimulations of 89 patients, we identified a total 188 (20.5%) left subcortical eloquent sites (in red), and 102 (11.1%) right subcortical eloquent sites (in blue). Each subcortical eloquent site identified intraoperatively using direct electrical stimulations in the depth of the surgical cavity is represented as a 5 mm in diameter region of interest in its actual position on a translucent brain according to the MNI 152 template. *A: anterior; L: left; R: right; S: superior*.

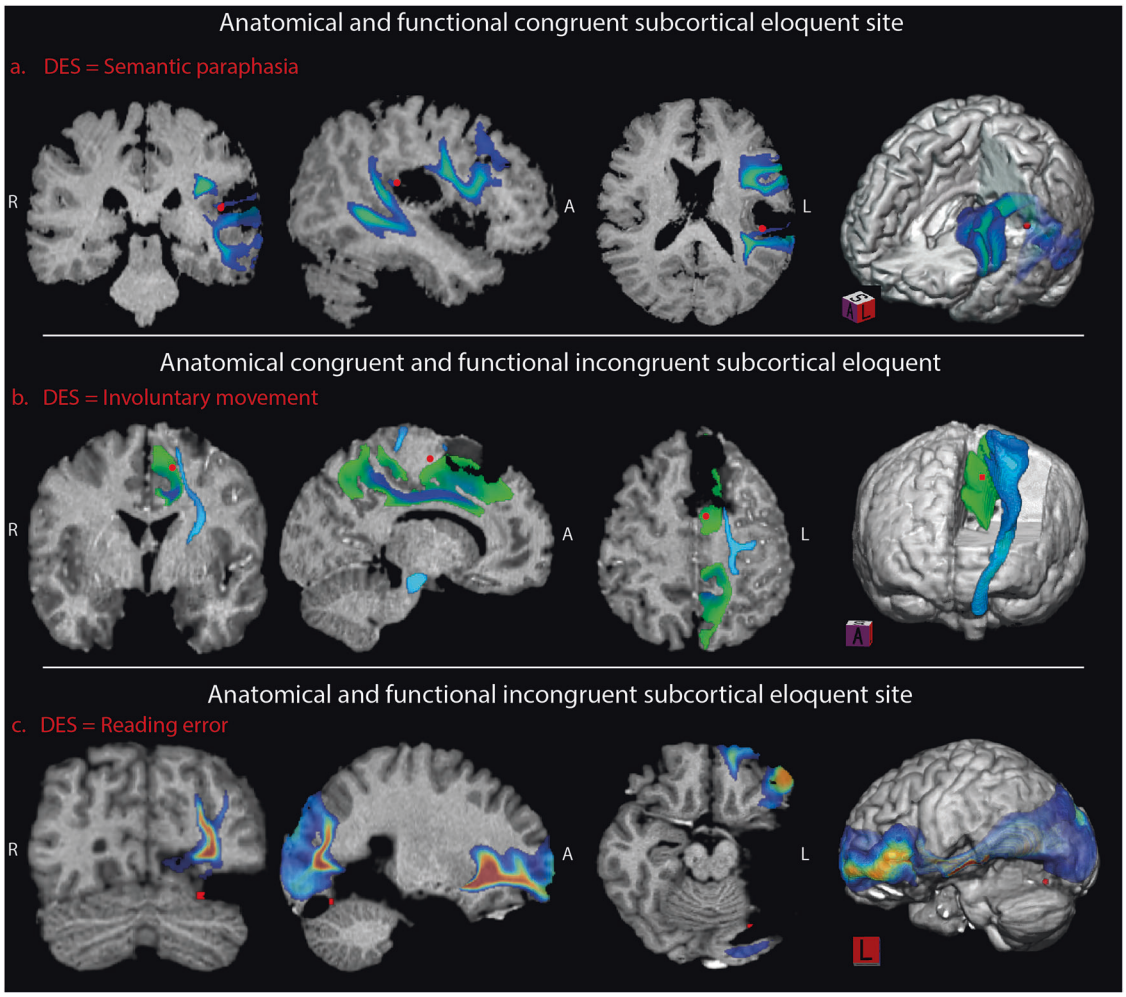

Fig. 3 | Illustrative cases of anatomical and functional adequacy /inadequacy. **a** *(top row)*: the red dot on the MNI 152 template represents an eloquent subcortical site identified intraoperatively during awake brain mapping corresponding to an elicited phonemic paraphasia (16) that is intersected with the left arcuate fasciculus, resulting in anatomical and functional congruence. Intraoperatively, the direct electrical stimulation of the dorsal phonological stream, including the arcuate fasciculus and the superior longitudinal fasciculus, elicites phonological errors during oral denomination in the awake patient. **b** *(middle row)*: the red dot on the MNI 152 template represents an eloquent subcortical site identified intraoperatively during awake brain mapping corresponding to an elicited semantic paraphasia (16) that is intersected with the left inferior fronto-occipital fasciculus, resulting in anatomical and functional congruence. Intraoperatively, the direct electrical stimulation of the ventral semantic stream, including the inferior fronto-occipital fasciculus, elicites semantic errors during oral denomination in the awake patient. **c** *(bottom row)*: the red dot on the MNI 152 template represents an eloquent subcortical site identified intraoperatively during awake brain mapping corresponding to an elicited involuntary movement (9) that is intersected with the corticospinal tract, resulting in an anatomical adequacy but a functional inadequacy. Intraoperatively, the direct electrical stimulation of the primary motor pathway elicites involuntary movement in the immobile awake patient. *A: anterior; DES: direct elicited site; L: left; R: right; S: superior*.

Validating the location of subcortical eloquent sites identified intraoperatively

The processed data to validate the identification of anatomical landmarks were qualified as "good" in 49/90 (54.4%) cases, as "medium" in 34/90 (37.8%) cases, and as "poor" in 7/90 (7.8%) cases. Cases with poor-quality processed data resulted from a postoperative MRI with surgically related artifacts (subdural air and blood) and did not significantly differ from cases with good-quality and medium-quality processed data regarding clinical-related, tumor-related, or surgery-related findings. In 1/7 cases with a poor-quality processed data, the alignment of the intraoperative photograph with the 3D model was not possible. This case was removed, resulting in 290 subcortical eloquent sites in 67/89 patients included in final analyses. The location of 271/290 (93.4%) subcortical eloquent sites were validated without change and the remaining 19/290 (6.6%) subcortical eloquent sites were re-adjusted. The degree of agreement between the observers was 93.4%. After accounting for chance agreement, Cohen's Kappa was 0.869, indicating a high level of agreement between the two observers.

Correlating intraoperative subcortical eloquent sites with reference white matter fiber tract atlas

Among the subcortical eloquent sites identified intraoperatively, 288/290 (99.3%) sites were successfully intersected with ≥1 white matter fiber tract according to the ICBM 2009a template independent of the brain functions sustained by the intersected white matter fiber tract. The 2/290 (0.7%) remaining subcortical eloquent sites did not interpolate with any white matter fiber tract. Among the subcortical eloquent sites that successfully intersected with ≥1 white matter fiber tract, 255/288 (88.5%) had a clinical response elicited intraoperatively that was congruent with one intersected white matter fiber tract. Characteristics of clinical responses elicited intraoperatively at subcortical eloquent points are detailed in Supplementary Table 3. In the remaining 33/288 (11.5%) subcortical eloquent sites that successfully intersected with ≥1 white matter fiber tract, the clinical response elicited intraoperatively was incongruent with any of the intersected white matter fiber tracts (Fig. 3). Details about the functional correlation between the subcortical eloquent sites and the elicited white

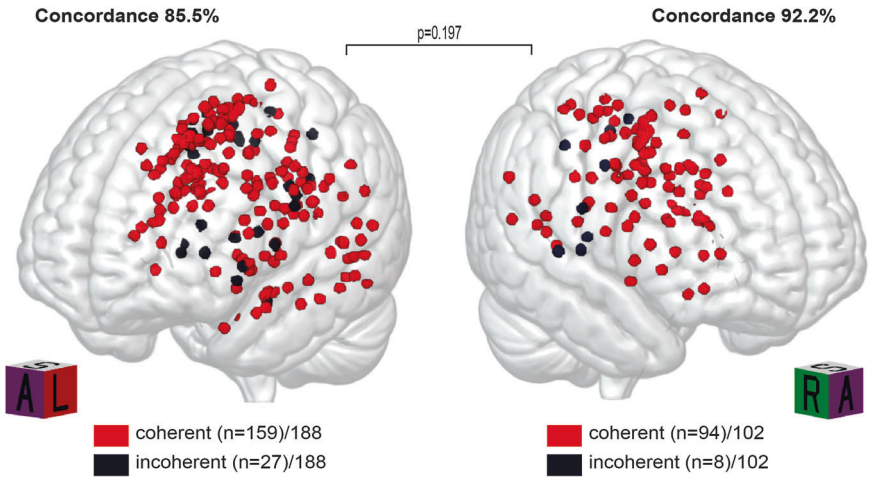

Fig. 4 | Overview of the functional congruence of all subcortical eloquent sites identified intraoperatively during awake brain mapping according to side ($n = 290$). Each subcortical eloquent site identified intraoperatively using direct electrical stimulations in the depth of the surgical cavity is represented as a 5 mm in diameter region of interest in its actual position on a translucent brain according to the MNI 152 template. *green dots:* functionally congruent subcortical eloquent sites. *red dots*: functionally incongruent subcortical eloquent sites. *A: anterior; L: left; R: right; S: superior.*

matter fiber tracts are detailed in Supplementary table 4. No significant difference according to hemispheric side was observed (left-side congruence 85.5%, right-side congruence 92.2%; $p = 0.197$) (Fig. 4). A 100% congruence between the clinical response elicited intraoperatively and the intersected white matter fiber tracts was observed for latencies during picture naming test ($n = 66/66$), dysarthria ($n = 9/9$), anarthria ($n = 8/8$), nonverbal semantic errors and emotion recognition errors ($n = 4/4$), reading errors ($n = 2/2$), perseverations during picture naming test ($n = 2/2$), dizziness ($n = 2/2$), and anomia ($n = 1/1$) (Supplementary fig. 6). A > 70% adequacy was observed for induced involuntary movements ($n = 65/72$, 89.0%), arrests of voluntary movements ($n = 56/57$, 98.2%), semantic paraphasia ($n = 35/37$, 94.6%), and phonemic paraphasia ($n = 28/33$, 84.8%). A ≤ 70% adequacy was observed for visual disorders ($n = 7/10$, 70.0%), phonological paraphasia ($n = 2/3$, 66.7%), and paresthesia ($n = 18/33$, 54.5%). Figure 5 illustrates subcortical eloquent sites eliciting a clinical response intraoperatively that were defined as congruent or incongruent with the intersected white matter fiber tracts.

The 35 subcortical eloquent sites identified intraoperatively that did not interpolate with a congruent white matter fiber tract, corresponded to the following clinical responses: paresthesia ($n = 15/35$, 42.9%), induced involuntary movements ($n = 8/35$, 22.9%), phonemic paraphasia ($n = 5/35$, 14.3%), visual disorders ($n = 3/35$, 8.6%), semantic paraphasia ($n = 2/35$, 5.7%), arrest of voluntary movements ($n = 1/35$, 2.8%), and phonological paraphasia ($n = 1/35$, 2.8%). Figure 6 represents the distance (mm) between the 35 incongruent subcortical eloquent sites and the stimulated white matter fiber tract according to the clinical response elicited intraoperatively. In these 35 sites, the minimal mean distance between the subcortical eloquent site and a congruent with matter fiber tract was 3.6 ± 4.4 mm (range 1.0–23.9, median 3.6, interquartile range 2.5–5.4) (Fig. 6). The longest distance was observed for the three subcortical eloquent sites eliciting visual disorders (mean 15.5 ± 8.7 mm, range 6.4–23.9, median 16.1, interquartile range 6.4–23.8), while the shortest distance was observed for the subcortical eloquent site eliciting arrests of unvoluntary movements (2.0 mm).

The complimentary analysis applying both a cutoff at 0.05 and at 0.01 to a random sample included 42 patients encompassing 181 subcortical eloquent sites (Supplementary data 2). Our results proved that the functional concordance between subcortical eloquent site and a congruent white matter fiber tract did not statistically differ considering a cutoff at 0.01 or at 0.05 ($p = 0.465$). A total of 155/181 (85.6%) and of 146/181 (80.1%) subcortical eloquent sites, respectively, having a clinical response elicited intraoperatively that was congruent with the intersected white matter fiber tract.

Discussion

We propose a step-by-step and detailed methodology to locate on a reference brain template the subcortical eloquent sites identified intraoperatively in the depth of the surgical cavity during functional brain mapping under awake conditions. We demonstrate that: 1) the imaging data processing was feasible in 89/90 (98.9%) patients; 2) 255/288 (88.5%) subcortical eloquent sites had a clinical response elicited intraoperatively that was congruent with the intersected white matter fiber tract; 3) in the 35 subcortical eloquent sites that did not successfully interpolate with a congruent white matter fiber tract, the minimal distance with a congruent with matter fiber tract ranged 1.0–23.9 mm.

We report a well-defined procedure to locate subcortical eloquent sites identified intraoperatively on a reference brain template aiming to standardize the methodology and results among research groups. Other research teams have previously proposed a methodology to locate the eloquent points identified intraoperatively on MRI[27,40–42]. According to previous reports in literature, we selected a homogeneous population of patients having the same surgical procedure (function-based awake resection) for the same brain tumor (supratentorial *IDH*-mutant diffuse glioma) to reduce variability, enhance statistical power validity and facilitate reproducibility. Our approach offers an improvement over previously reported methodologies that rely on intraoperative and postoperative MRI localization techniques. Notably, Ng et al. [40,42]. used normalized MRIs to identify the position of eloquent sites identified intraoperatively by visually aligning to an approximate template, assessing intra- and inter-observer agreement based on these approximations. However, a critical limitation of this approach is the loss of individual anatomical details due to template normalization, which diminishes the specificity of patient-specific anatomy. The normalization process significantly deforms cortical and subcortical regions, which are inherently less reliably aligned to a template, particularly in relation to preoperative imaging and intraoperative anatomy. The same research group attempted to improve the location of eloquent sites identified intraoperatively through a "pial mesh" model derived from postoperative MRI three months after surgery, analogous to our 3D model approach based on early postoperative MRI[41]. While promising, this method suffers from the following limitation: the post-surgical cavity undergoes extensive remodeling within this timeframe, resulting in distortions that limit the accuracy of eloquent site location in comparison to intraoperative anatomical landmarks. This highlights the advantage of the present method, which seeks to preserve the integrity of individual anatomy throughout the process, enhancing the fidelity of subcortical site localization by prioritizing intraoperative data. Furthermore, Lu et al. [27]. mapped eloquent sites identified intraoperatively on a hand-drawn brain template, subsequently digitized and adapted to the MNI template. Their method involved calculating and applying a deformation index to align hand-drawn and digital points to a standardized space, similar to our own deformation-based adjustments. However, this approach introduces variability in anatomical fidelity due to the use of two different models prior to normalization, underscoring the need for high anatomical accuracy in direct electrode positioning. We

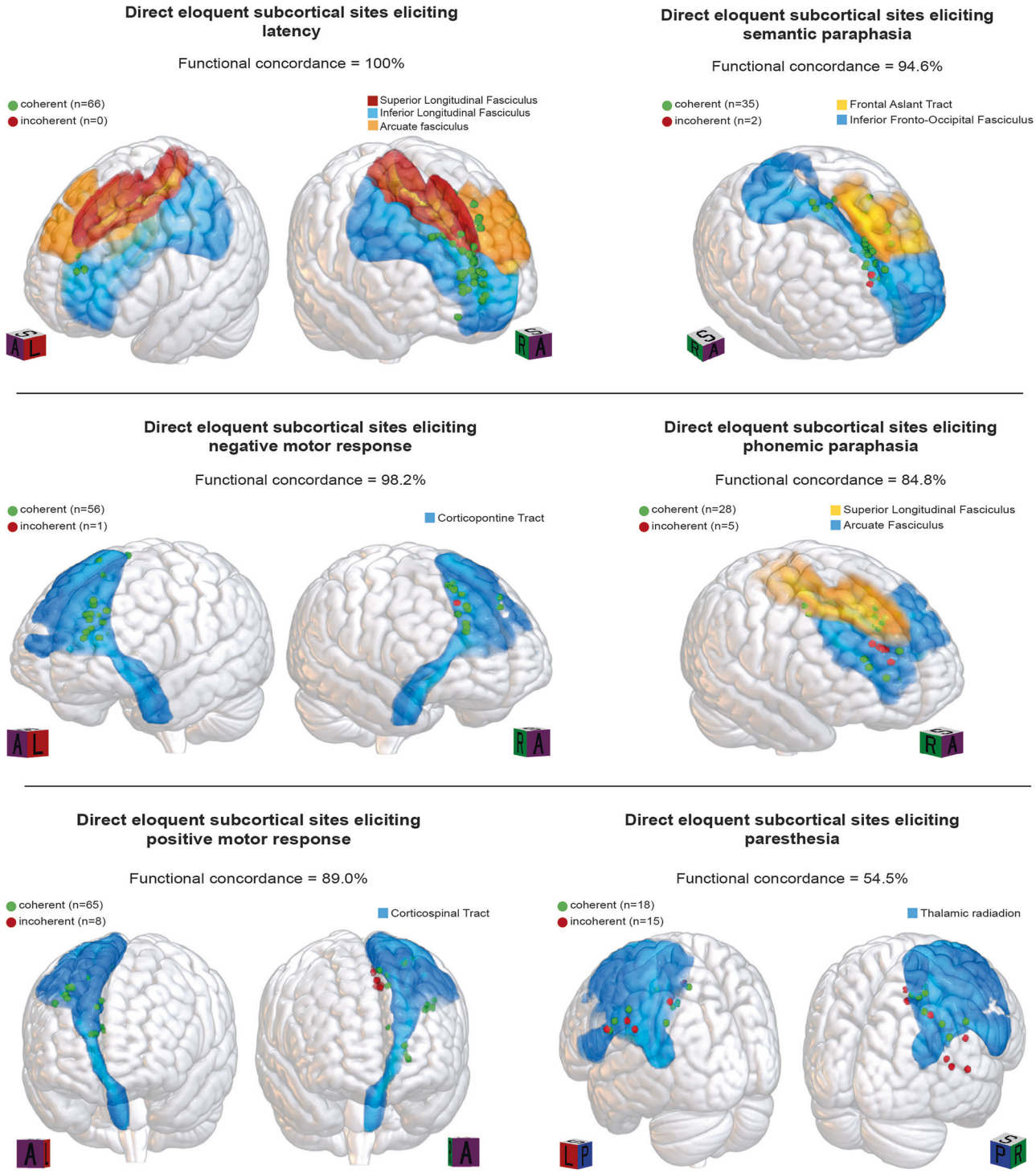

Fig. 5 | Illustrative overview of subcortical eloquent sites identified intraoperatively during awake brain mapping according to the elicited clinical responses and to the intersected white matter fiber tracts. Each subcortical eloquent site identified intraoperatively using direct electrical stimulations in the depth of the surgical cavity is represented as a 5 mm in diameter region of interest in its actual position on a translucent brain according to the MNI 152 template. *Green dots:* functionally congruent subcortical eloquent sites. *Red dots:* functionally incongruent subcortical eloquent sites. *A: anterior; L: left; R: right; S: superior.*

ensured the accuracy of the normalization procedure by demonstrating the low distance of reference points between normalized images and the reference MNI template, with a margin of error similar than those previously reported[38,43–45]. With the full knowledge of the limitations of comparing the individual brain connections identified intraoperatively using direct electrical stimulations with a statistical tractography atlas according to the HCP atlas from healthy patients, we ensured the proper anatomical location of each subcortical eloquent sites identified intraoperatively by correlating them with white matter fiber tracts using MNI brain template. We reported a functional concordance of 88.5% between the tractography atlas and the subcortical eloquent sites identified intraoperatively. We observed that for easy to record clinical responses elicited intraoperatively by direct electrical stimulations (anarthria, anomia and dysarthria), the functional concordance rose up to 100%. Conversely, for more subjective and patient-dependent clinical responses elicited intraoperatively (paresthesia, visual disorder), the functional concordance was ≤70%. This underlines

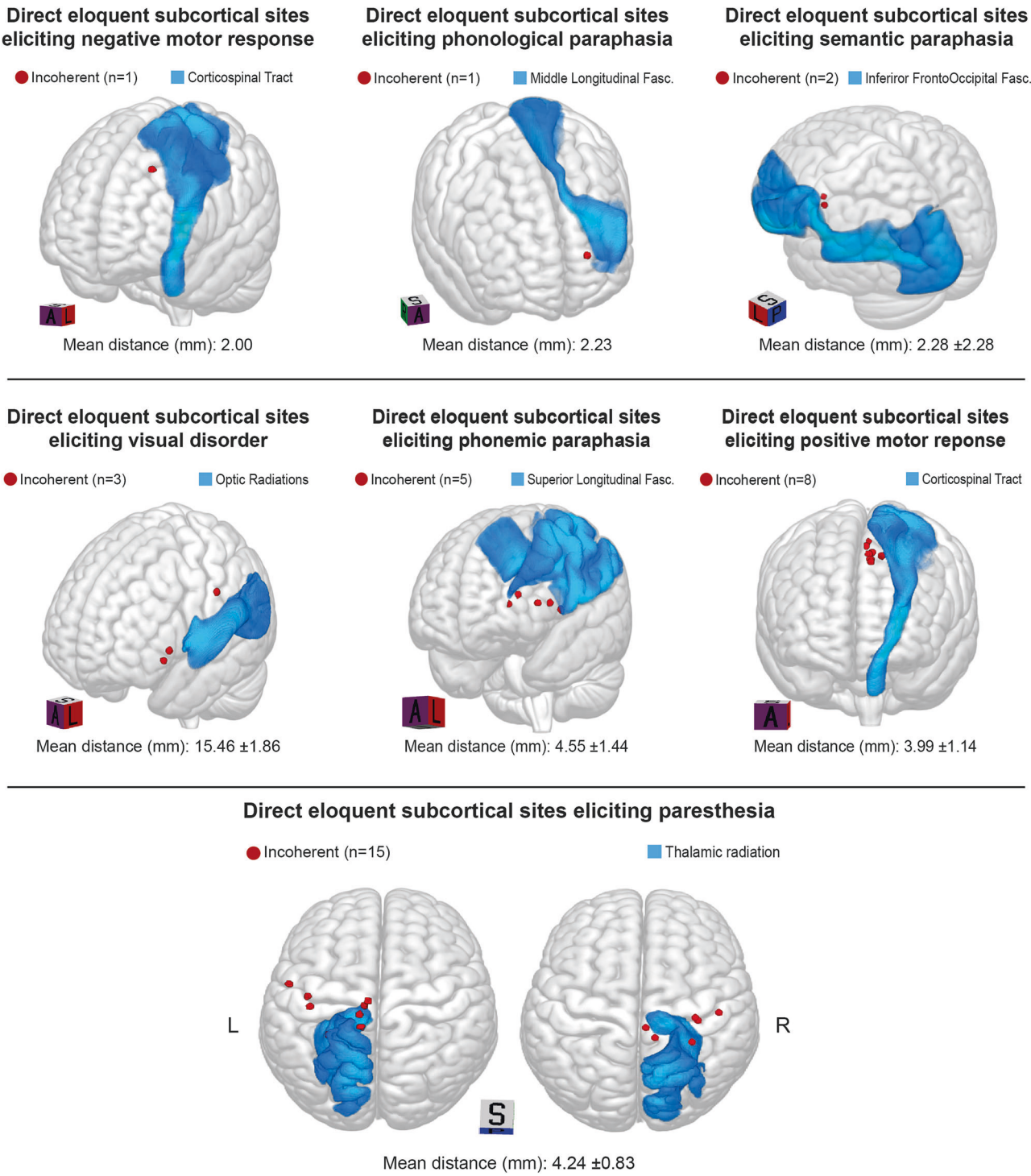

Fig. 6 | Illustrative overview of the 35 subcortical eloquent sites identified intraoperatively that did not interpolate with a congruent white matter fiber tract. Detailed distance (mm) between each incongruent subcortical eloquent site identified intraoperatively during awake brain mapping and the closest congruent white matter fiber tract according to the elicited clinical response. Each subcortical eloquent site identified intraoperatively using direct electrical stimulations in the depth of the surgical cavity is represented as a 5 mm in diameter region of interest in its actual position on a translucent brain according to the MNI 152 template. *A: anterior; L: left; R: right; S: superior*.

how the patient's cooperation, the proper selection of intraoperative tasks, and the experience of the speech therapist, are essential to achieve an efficient intraoperative brain mapping[1,2,4,12,14,33,34,46–48]. In addition, in cases of subcortical eloquent sites not intersecting with a congruent white matter fiber tract, the distance between the subcortical eloquent site and a congruent with matter fiber tract was short (mean 3.6 ± 4.4 mm). This may correspond to: 1) inaccuracy during imaging data processing; 2) current diffusion during direct electrical stimulations, and 3) the observation of glioma-induced brain plasticity, the actual white matter fiber tracts identified intraoperatively on patients differing of reference brain atlases from healthy controls. The longest distance was observed for subcortical eloquent sites eliciting visual disorders intraoperatively, in which the patient reported non-specific "visual problems" that were not possible to objectively verify and forcibly attributed to the stimulation of the optic radiations in our

research methodology. A significant issue in locating a subcortical eloquent site identified intraoperatively on a reference template is to properly quantify the volume of the stimulated brain. Several factors play a role during the identification of white matter tracts using direct electrical stimulations: 1) those related to the stimulation parameters (probe, pulse frequency, amplitude, polarity, phase); 2) those related to the application of the stimulation (probe geometry, orientation of the probe compared to the orientation of the white matter fiber tract, duration, tissue conductivity); 3) those related to the interactions between the tumor and the white matter fiber tracts (distortion, infiltration, interruption, brain deformation, edema)[49–52]; and 4) those related to glioma-induced brain plasticity (compensation, reshaping, and rewiring of brain connections)[6]. To control for these possible biases, we modelized a subcortical eloquent site as a 5 mm in diameter sphere. This represented a physical approximation of the electrical field applied intraoperatively to the brain during the awake functional mapping that depended on parameters detailed above[49–52]. This approximation covered the most possible combinations of all stimulation parameters and so all eventual scenarios during intraoperative awake functional brain mapping. Moreover, this model recalls those applied in previous studies using similar brain stimulation procedures and parameters[49–55].

The present study proposed a validated and standardized methodology for locating subcortical eloquent subcortical sites identified intraoperatively using direct electrical stimulations during awake brain mapping on a reference brain template. We selected a homogeneous population of adult patients harboring the same brain lesion who underwent the same awake procedure conducted by the same senior neurosurgeon. Contrarily to neuronavigation-based co-registrations attempts based on preoperative MRI with inherent biases induced by intraoperative brain shift[31], we took advantage of the brain shift and controlled for it by using the early postoperative MRI that usually shows a brain shift comparable to those encountered at the end of the resection. This transient brain shift, visible on both intraoperative 2D photographs and on 3D brain reconstruction of the early postoperative MRI, helped the co-registrations between these two modalities. We used the early postoperative MRI for imaging data processing to ensure a correct overlay between intraoperative photographs and surgical cavity. We controlled for surgery-related artefacts that affected the quality of the surface rendering using quality control assessments. The choice of a longer-term postoperative MRI would have allowed better volume rendering with less postoperative artefacts but with more shift and retraction of the surgical cavity, precluding the accurate overlay of the subcortical eloquent sites on the resection cavity. The present methodology can be applied to all studies correlating neuroimaging data with intraoperative functional data obtained using direct electrical stimulations and could help: 1) locating subcortical eloquent sites identified intraoperatively on a reference brain template; 2) proposing a reproducible procedure to standardize the research methodology using direct electrical stimulations to study brain connectivity. In this study, we focused exclusively on the same neoplasm (*IDH*-mutant glioma) and on the same neurosurgical procedure to enhance reproducibility and reduce biological heterogeneity. Beyond gliomas, this approach could be extended to any enduring brain lesion located within eloquent areas and requiring function-based awake resection using cortico-subcortical mapping.

Limitations arising from data collection include the retrospective design, the single-center setting, intraoperative photographs obtained using different machines, and the subjective recording of clinical responses elicited intraoperatively by direct electrical stimulations on a clinical basis by a senior speech therapist. The presence of glioma- and surgery-induced brain shift may have limited the normalization procedure. To control for this bias, we used previously reported and validated nonlinear transformation methods[38]. Among them, SPM12's Clinical Toolbox normalization is well-regarded for handling brain MRIs with lesions, largely due to the integration of Tissue Probability Maps that provide a reference framework based on standard tissue distributions, which helps improve the accuracy of lesion normalization by aligning the lesion-affected areas to a common template, conversely to the enantiomorphic or the cost mask function normalization. The human interventions during pre-processing phases (parameter adjustment in MANGO, co-registration between 2D intraoperative photographs onto 2D projection of the 3D brain reconstruction) involve gaining expertise over time and may have induced errors in allocating eloquent subcortical sites. We have developed a methodology which allowed to visually identify anatomical landmarks during overlay process and assess the level of quality. With the determination of multiple quality assessments by two investigators and the same assessment carried out by the same two investigators, we may create a systematic error but eliminate randomized errors, therefore resulting in an accurate methodology for the location on reference brain template of eloquent subcortical areas identified intraoperatively. We controlled the biases related to intraoperative functional brain mapping using direct electrical stimulations by a physical approximation of the volume of stimulated brain in accordance with previous reports[6,20,26,27,49,50,52]. One major limitation in this research is the direct co-registration of the subcortical eloquent sites with the expected brain connectivity on a brain tract atlas instead of patient's specific DTI. We chose this option because DTI data: 1) require extensive post-processing limiting its availability, particularly in large-scale clinical studies; 2) are sensitive to a variety of factors, including motion artifacts, noise, and image distortion, which can complicate data acquisition and interpretation in the specific condition of brain neoplasms; 3) of each patient has to be normalized to a common brain atlas, which may introduce further variability in results. While tractography provides valuable insights into white matter connectivity, it is important to acknowledge its inherent limitations. One of the primary concerns is the potential for both false-positive and false-negative connections, due to the inherent smoothing and probabilistic nature of fiber reconstruction and difficulties in resolving crossing, kissing, or branching fibers, particularly in areas of complex white matter architecture. Indeed, the ICBM 2009a template, determined on healthy subjects, does not integrate glioma-induced brain plasticity and mass effect that may have rewired the brain connections of patients under study. This may have affected, together with the parameters under study, the possibility of correspondence between eloquent subcortical sites eliciting a clinical response intraoperatively and white matter pathways of the ICBM 2009a template. This, therefore, not only may serve as an explanation of some subcortical eloquent sites not corresponding to a white matter fiber tract but may also be a qualitative and quantitative demonstration of how re-organization of brain connections occurs in patients with an *IDH*-mutant glioma. Here, we attempted to mitigate these limitations by adopting a low voxel threshold (0.01) to enhance sensitivity while reducing spurious tracts. In addition, we performed a sensitivity analysis with a more conservative threshold (0.05) to ensure the robustness of the findings. It is important to recognize that tractography does not represent an absolute gold standard for white matter mapping and errors in fiber tracking may have influenced the present results. Another limitation is the use of rigid registration to co-register intraoperative photographs with early postoperative MRI. We used MRI within 48 h post-surgery, a timeframe in which brain shift is expected to be minimal compared to delayed imaging. We acknowledge that residual deformations may still occur, potentially affecting the accuracy of subcortical eloquent site location. While rigid registration assumes a fixed anatomical relationship between intraoperative and postoperative images, it does not account for these deformations. Non-rigid registration techniques, which allow for local deformations, could provide a more refined alignment, particularly in cases with significant brain shift related to longer term postoperative MRI. However, implementing such methods requires a careful balance between improved spatial accuracy and potential interpolation artifacts introduced by deformable transformations. Ultimately, the development of hybrid approaches combining rigid and non-rigid registration may offer an optimized solution to enhance spatial fidelity without introducing excessive computational complexity. These findings should be interpretated with the knowledge of the limitations and further

confirmatory analyses, incorporating *IDH*-wildtype gliomas and other brain lesions in an external dataset, are required to reproduce the results and to ensure the validity and the usefulness of the proposed methodology.

We proposed a standardized methodology to locate subcortical eloquent sites identified intraoperatively during functional brain mapping using direct electrical stimulations under awake condition on a reference brain template. The methodology was able to determine a functional concordance between subcortical eloquent sites identified intraoperatively and MNI reference brain template in 88.5%. This may help incorporating functional data obtained with direct electrical stimulations during awake surgery in the methodological workup to study brain connectivity.

Data availability

Clinical data is owned by GHU Paris Sainte-Anne and is not freely available due to patient privacy and confidentiality regulations. Access to this data can be granted by submitting a completed request form, in compliance with institutional protocols and ethical guidelines. Additionally, two supplementary files are available for further reference: Supplementary data 1 reports a quantitative analysis by evaluating the agreement between the blinded evaluators' identification of the same points on normalized brains; Supplementary data 2 reports a complimentary analysis applying both a cutoff at 0.05 and at 0.01 to a random sample of 42 patients encompassing 181 subcortical eloquent sites.

Code availability

The MATLAB code used in this study is an intellectual property of the authors. It will be made available upon reasonable request from the corresponding author (J.P.).

Abbreviation

HCP	Human Connectome Project
GUI	Graphical User Interface
ICBM	International Consortium for Brain Mapping
IDH	Isocitrate Dehydrogenase
IRB	Institutional Review Board
MANGO	Multi-image Analysis Graphical User Interface
MNI	Montreal Neurological Institute
MRI	Magnetic Resonance Imaging
NIFTI	Neuroimaging Informatics Technology Initiative
ROI	Region Of Interest
SPM	Statistical Parametric Mapping

Received: 7 November 2024; Accepted: 10 March 2025;
Published online: 07 May 2025

References

1. Pallud, J. et al. Surgery of Insular Diffuse Gliomas-Part 1: Transcortical Awake Resection Is Safe and Independently Improves Overall Survival. *Neurosurgery* **89**, 565–578 (2021).
2. Elia, A. et al. A Preoperative Scoring System to Predict Function-Based Resection Limitation Due to Insufficient Participation During Awake Surgery. *Neurosurgery* **93**, 678–690 (2023).
3. Coletta, L. et al. Integrating direct electrical brain stimulation with the human connectome. *Brain* https://doi.org/10.1093/brain/awad402 (2023).
4. Pallud, J. et al. Direct electrical bipolar electrostimulation for functional cortical and subcortical cerebral mapping in awake craniotomy. Practical considerations. *Neurochirurgie* **63**, 164–174 (2017).
5. Zanello, M. et al. Predictors of early postoperative epileptic seizures after awake surgery in supratentorial diffuse gliomas. *J. Neurosurg.* **134**, 683–692 (2020).
6. Ng, S., Duffau, H. & Herbet, G. Perspectives in human brain plasticity sparked by glioma invasion: from intraoperative (re)mappings to neural reconfigurations. *Neural Regen. Res.* **19**, 947–948 (2024).
7. Prat-Acín, R., Galeano-Senabre, I., López-Ruiz, P., Ayuso-Sacido, A. & Espert-Tortajada, R. Intraoperative brain mapping of language, cognitive functions, and social cognition in awake surgery of low-grade gliomas located in the right non-dominant hemisphere. *Clin. Neurol. Neurosurg.* **200**, 106363 (2021).
8. McCarty, M. J. et al. Intraoperative cortical localization of music and language reveals signatures of structural complexity in posterior temporal cortex. *iScience* **26**, 107223 (2023).
9. Duffau, H. et al. Usefulness of intraoperative electrical subcortical mapping during surgery for low-grade gliomas located within eloquent brain regions: functional results in a consecutive series of 103 patients. *J. Neurosurg.* **98**, 764–778 (2003).
10. Ghimire, P. et al. Intraoperative mapping of pre-central motor cortex and subcortex: a proposal for supplemental cortical and novel subcortical maps to Penfield's motor homunculus. *Brain Struct. Funct.* **226**, 1601–1611 (2021).
11. Pallud, J. et al. Surgery of Insular Diffuse Gliomas-Part 2: Probabilistic Cortico-Subcortical Atlas of Critical Eloquent Brain Structures and Probabilistic Resection Map During Transcortical Awake Resection. *Neurosurgery* **89**, 579–590 (2021).
12. Muto, J. et al. Functional-Based Resection Does Not Worsen Quality of Life in Patients with a Diffuse Low-Grade Glioma Involving Eloquent Brain Regions: A Prospective Cohort Study. *World Neurosurg* **113**, e200–e212 (2018).
13. Pelletier, J.-B. et al. Is function-based resection using intraoperative awake brain mapping feasible and safe for solitary brain metastases within eloquent areas? *Neurosurg. Rev.* **44**, 3399–3410 (2021).
14. Moiraghi, A. et al. Feasibility, Safety and Impact on Overall Survival of Awake Resection for Newly Diagnosed Supratentorial IDH-Wildtype Glioblastomas in Adults. *Cancers (Basel)* **13**, 2911 (2021).
15. De Witt Hamer, P. C., Robles, S. G., Zwinderman, A. H., Duffau, H. & Berger, M. S. Impact of Intraoperative Stimulation Brain Mapping on Glioma Surgery Outcome: A Meta-Analysis. *J. Clin. Oncol.* **30**, 2559–2565 (2012).
16. Smith, J. S. et al. Role of Extent of Resection in the Long-Term Outcome of Low-Grade Hemispheric Gliomas. *J. Clin. Oncol.* **26**, 1338–1345 (2008).
17. Caverzasi, E. et al. Identifying preoperative language tracts and predicting postoperative functional recovery using HARDI q-ball fiber tractography in patients with gliomas. *J. Neurosurg.* **125**, 33–45 (2016).
18. Sanai, N. & Berger, M. S. Surgical oncology for gliomas: the state of the art. *Nat. Rev. Clin. Oncol.* **15**, 112–125 (2018).
19. Freyschlag, C. F. & Duffau, H. Awake brain mapping of cortex and subcortical pathways in brain tumor surgery. *J. Neurosurg. Sci.* **58**, 199–213 (2014).
20. Duffau, H. What direct electrostimulation of the brain taught us about the human connectome: a three-level model of neural disruption. *Front. Hum. Neurosci*. **14**, 315 (2020).
21. Margolis, D. J. et al. Reorganization of cortical population activity imaged throughout long-term sensory deprivation. *Nat. Neurosci.* **15**, 1539–1546 (2012).
22. Küpper, H. et al. Comparison of Different Tractography Algorithms and Validation by Intraoperative Stimulation in a Child with a Brain Tumor. *Neuropediatrics* **46**, 072–075 (2014).
23. Li, Y. et al. Diffusion tensor imaging versus intraoperative subcortical mapping for glioma resection: a systematic review and meta-analysis. *Neurosurg. Rev.* **46**, 154 (2023).
24. Kang, K. M. et al. Functional Magnetic Resonance Imaging and Diffusion Tensor Imaging for Language Mapping in Brain Tumor Surgery: Validation With Direct Cortical Stimulation and Cortico-Cortical Evoked Potential. *Korean J. Radiol.* **24**, 553–563 (2023).

25. Tate, M. C., Herbet, G., Moritz-Gasser, S., Tate, J. E. & Duffau, H. Probabilistic map of critical functional regions of the human cerebral cortex: Broca's area revisited. *Brain* **137**, 2773–2782 (2014).
26. Chang, E. F. et al. Stereotactic probability and variability of speech arrest and anomia sites during stimulation mapping of the language dominant hemisphere. *J. Neurosurg.* **126**, 114–121 (2017).
27. Lu, J. et al. Functional maps of direct electrical stimulation-induced speech arrest and anomia: a multicentre retrospective study. *Brain* **144**, 2541–2553 (2021).
28. Sarubbo, S. et al. Mapping critical cortical hubs and white matter pathways by direct electrical stimulation: an original functional atlas of the human brain. *Neuroimage* **205**, 116237 (2020).
29. Wu, J. et al. Direct evidence from intraoperative electrocortical stimulation indicates shared and distinct speech production center between Chinese and English languages. *Hum. Brain Mapp.* **36**, 4972–4985 (2015).
30. Corrivetti, F. et al. Dissociating motor–speech from lexico-semantic systems in the left frontal lobe: insight from a series of 17 awake intraoperative mappings in glioma patients. *Brain Struct. Funct.* **224**, 1151–1165 (2019).
31. Bayer, S., Maier, A., Ostermeier, M. & Fahrig, R. Intraoperative Imaging Modalities and Compensation for Brain Shift in Tumor Resection Surgery. *Int. J. Biomed. Imaging* **2017**, 1–18 (2017).
32. Louis, D. N. et al. The 2021 WHO Classification of Tumors of the Central Nervous System: a summary. *Neuro. Oncol.* **23**, 1231–1251 (2021).
33. Pallud, J. et al. Surgery of Insular Diffuse Gliomas—Part 1. *Neurosurgery* **89**, 565–578 (2021).
34. Pallud, J. et al. Technical principles of direct bipolar electrostimulation for cortical and subcortical mapping in awake craniotomy. *Neurochirurgie* **63**, 158–163 (2017).
35. Herbet, G., Rigaux-Viodé, O. & Moritz-Gasser, S. Peri- and intraoperative cognitive and language assessment for surgical resection in brain eloquent structures. *Neurochirurgie* **63**, 135–141 (2017).
36. Gil-Robles, S. & Duffau, H. Surgical management of World Health Organization Grade II gliomas in eloquent areas: the necessity of preserving a margin around functional structures. *Neurosurg. Focus* **28**, E8 (2010).
37. Arizona.edu, D. P. P. D. dkp @. SPM12 Revised Normalization. https://neuroimaging-core-docs.readthedocs.io/en/latest/pages/spm_anat_normalization-rev.html.
38. Roux, A. et al. MRI Atlas of IDH Wild-Type Supratentorial Glioblastoma: Probabilistic Maps of Phenotype, Management, and Outcomes. *Radiology* **293**, 633–643 (2019).
39. Fonov, V., Evans, A., McKinstry, R., Almli, C. & Collins, D. Unbiased nonlinear average age-appropriate brain templates from birth to adulthood. *Neuroimage* **47**, S102 (2009).
40. Roux, A. et al. Combining Electrostimulation With Fiber Tracking to Stratify the Inferior Fronto-Occipital Fasciculus. *Front. Neurosci*. **15**, 683348 (2021).
41. Ng, S., Moritz-Gasser, S., Lemaitre, A.-L., Duffau, H. & Herbet, G. White matter disconnectivity fingerprints causally linked to dissociated forms of alexia. *Commun. Biol.* **4**, 1413 (2021).
42. Ng, S. et al. Intraoperative functional remapping unveils evolving patterns of cortical plasticity. *Brain* **146**, 3088–3100 (2023).
43. Ripollés, P. et al. Analysis of automated methods for spatial normalization of lesioned brains. *Neuroimage* **60**, 1296–1306 (2012).
44. Klein, A. et al. Evaluation of 14 nonlinear deformation algorithms applied to human brain MRI registration. *Neuroimage* **46**, 786–802 (2009).
45. Crinion, J. et al. Spatial normalization of lesioned brains: Performance evaluation and impact on fMRI analyses. *Neuroimage* **37**, 866–875 (2007).
46. Gogos, A. J., Young, J. S., Morshed, R. A., Hervey-Jumper, S. L. & Berger, M. S. Awake glioma surgery: technical evolution and nuances. *J. Neurooncol.* **147**, 515–524 (2020).
47. Hervey-Jumper, S. L. et al. Awake craniotomy to maximize glioma resection: methods and technical nuances over a 27-year period. *J. Neurosurg.* **123**, 325–339 (2015).
48. Pallud, J. & Dezamis, E. Surgical resection in eloquent brain regions – introduction. *Neurochirurgie* **63**, 115–116 (2017).
49. Schlosser-Perrin, F., Rossel, O., Duffau, H., Bonnetblanc, F. & Mandonnet, E. How far does electrical stimulation activate white matter tracts? A computational modeling study. *Clin. Neurophysiol.* **153**, 68–78 (2023).
50. Dali, M., Goldman, J. S., Pantz, O., Destexhe, A. & Mandonnet, E. Modeling subcortical white matter stimulation. *bioRxiv* https://doi.org/10.1101/2019.12.12.872390 (2019).
51. Shiban, E. et al. Intraoperative subcortical motor evoked potential stimulation: how close is the corticospinal tract? *J. Neurosurg.* **123**, 711–720 (2015).
52. Szelényi, A. et al. Intra-operative subcortical electrical stimulation: A comparison of two methods. *Clin. Neurophysiol.* **122**, 1470–1475 (2011).
53. Nossek, E. et al. Intraoperative mapping and monitoring of the corticospinal tracts with neurophysiological assessment and 3-dimensional ultrasonography-based navigation. *J. Neurosurg.* **114**, 738–746 (2011).
54. Ozawa, N., Muragaki, Y., Nakamura, R., Hori, T. & Iseki, H. Shift of the Pyramidal Tract During Resection of the Intraaxial Brain Tumors Estimated by Intraoperative Diffusion-Weighted Imaging. *Neurol. Med. Chir. (Tokyo)* **49**, 51–56 (2009).
55. Berman, J. I., Berger, M. S., Chung, S., Nagarajan, S. S. & Henry, R. G. Accuracy of diffusion tensor magnetic resonance imaging tractography assessed using intraoperative subcortical stimulation mapping and magnetic source imaging. *J. Neurosurg.* **107**, 488–494 (2007).

Author contributions

Conceptualization: J.P. Methodology: A.E., and J.P. Investigation: A.E., A.R., C.D., S.C., GS., A.M., B.T., E.D., J.M., F.C., M.Z., CO. and J.P. Visualization: A.E., A.R., C.D., S.C., and J.P. Funding acquisition: J.P. Project administration: J.P. Supervision: J.P. Writing – original draft: A.E., and J.P. Writing – review & editing: A..E., A.R., C.D., S.C., G.S., A.M., B.T., E.D., J.M., F.C., M.Z., C.O. and J.P.

Competing interests

The authors declare no competing interests.

Additional information

Supplementary information The online version contains supplementary material available at https://doi.org/10.1038/s43856-025-00834-6.

Correspondence and requests for materials should be addressed to Johan Pallud.

Peer review information *Communications Medicine* thanks Gabriele Amorosino, Mehrnaz Jenabi and Yuyao Zhou for their contribution to the peer review of this work. Peer review reports are available.